Evaluation of Pore Structure in Pure Silica Zeolite MFI Low-*k* Thin Films Using Positronium Annihilation Lifetime Spectroscopy

Shuang Li,[†] Jianing Sun,[‡] Zijian Li,[†] Huagen Peng,[‡] David Gidley,[§] E. Todd Ryan,[⊥] and Yushan Yan*,[†]

Department of Chemical and Environmental Engineering, University of California, Riverside, California 92521; Department of Materials Science and Engineering, University of Michigan, Ann Arbor, Michigan 48109; Department of Physics, University of Michigan, Ann Arbor, Michigan 48109; and Advanced Micro Devices, IBM East Fishkill, Hopewell Junction, New York 12533

Received: March 23, 2004; In Final Form: May 27, 2004

The pore size and pore structure in pure silica zeolite MFI in-situ and spin-on low dielectric constant (low-*k*) zeolite films were characterized by positronium annihilation lifetime spectroscopy (PALS). For the micropores in the in-situ and spin-on films, the pore size obtained from the on-wafer PALS method is 0.55 ± 0.03 nm, and this is in excellent agreement with the known crystallographically determined zeolitic pore size (0.55 nm). To our knowledge this is the first comparison of a PALS thin film pore size measurement with a crystallographically defined zeolite pore size. For mesopores in the spin-on film, PALS results show that they are open/interconnected and give a pore size of 2.3−2.6 nm.

Introduction

Higher conductivity metals and lower dielectric constant (low-*k*) insulators are required to overcome the signal delay and cross-talk noise problems for future generation computer microprocessors.[1−4] While the semiconductor industry has adopted copper in place of aluminum for the metal wires, the implementation of low-*k* materials that meet the stringent integration and reliability requirements of high-performance microprocessors has been more difficult and slower than expected. Studies show that ultralow-*k* ($k < 2.2$) materials are necessary for future microprocessors, and for most materials porosity is necessary to achieve $k < 2.5$.[2] However, increasing porosity reduces the mechanical strength and heat conductivity of the films.[5]

We have reported that zeolites are promising low-*k* materials, and a key advantage of zeolite-based low-*k* materials is the ability to lower *k* while maintaining much higher mechanical strength than other amorphous porous low-*k* materials.[6,7] Zeolites are a type of microporous crystalline materials with uniform molecular sized pores. In our previous study, pure silica zeolite (PSZ) MFI low-*k* films were prepared by spin-on as well as in-situ crystallization methods. The in-situ crystallized zeolite films have only one level of porosity—the intrinsic zeolitic micropores—and this makes in-situ zeolite films an ideal system to study the intrinsic properties of a zeolite film and the effect of zeolite framework density on its dielectric properties. On the other hand, spin-on films from zeolite nanoparticle suspensions were also developed to take advantage of both the intrinsic zeolite microporosity and the interparticle mesoporosity.

Since pore volume, pore size, pore size distribution, and pore interconnectivity strongly affect the dielectric properties, characterization of pore structure in porous films is crucial for their application as low-*k* materials.[8] To obtain such information for zeolite films, we used N_2 adsorption measurements on bulk silica samples that structurally resemble the films in our previous studies. Specifically, we measured bulk MFI crystals collected from in-situ syntheses and silica obtained by drying the nanoparticle suspension for the spin-on films. A very good correlation was obtained between the measured *k* values of the films and the theoretical *k* values predicted from the measured total porosity of the bulk material by N_2 adsorption based on Bruggeman's model.[6]

Although gas absorption has been useful to measure surface area, pore volume, pore size, and pore size distribution of powdery samples, it has limitations in measuring porosity of a supported thin film where the amount of available adsorbent is usually too small. As a result, a large number of coated wafers are needed, and the films have to be scratched off from the wafers. This means that nitrogen adsorption will remain an off-wafer and destructive method. In addition, the nitrogen adsorption method cannot detect closed pores due to the inaccessibility of these pores to the gas molecules and thus cannot give pore connectivity information even though this information is very important in determining important properties of the low-*k* films such as moisture sensitivity and thermal conductivity.

Recently, several nondestructive on-wafer methods such as positronium annihilation lifetime spectroscopy (PALS), small-angle neutron scattering spectroscopy combined with specular X-ray reflectivity (SANS−SXR), and ellipsometric porosimetry (EP) have been developed to determine the porosity, pore size, and pore size distribution of low-*k* porous thin films.[8−10] These techniques are based on different physical principles. In the SANS−SXR method,[11] SXR is used to measure the thickness and the density of the film while SANS provides data related to pore wall density and porosity. The data from SXR and SANS are combined to calculate pore size and porosity. Deuterated toluene can be used as adsorbate in the SANS measurements to probe the pore connectivity. EP is a method that relies on the optical property change of a film during the adsorption and

* To whom correspondence should be addressed. E-mail: Yushan.Yan@ucr.edu.
[†] University of California, Riverside.
[‡] Department of Materials Science and Engineering, University of Michigan.
[§] Department of Physics, University of Michigan.
[⊥] IBM East Fishkill.

10.1021/jp048707l CCC: $27.50
Published on Web 07/13/2004

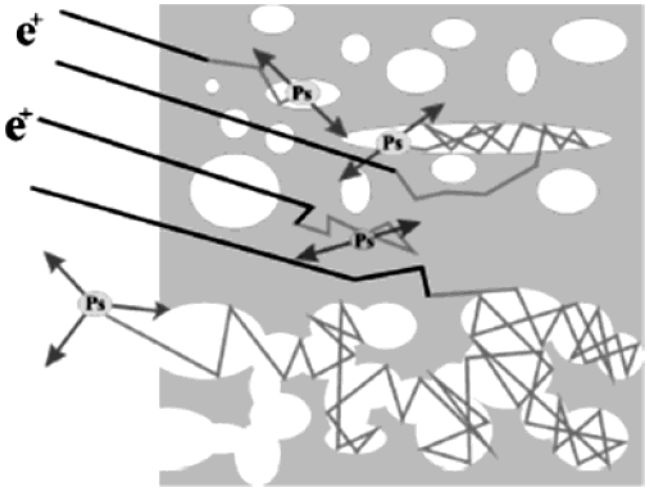

Figure 1. Positronium behavior in two types of porous materials: (upper) closed pores and (lower) connected pores.

desorption of an adsorbate. Toluene is commonly used as the adsorbate. The analysis of the desorption isotherms to obtain pore size, pore size distribution, and porosity is similar to nitrogen adsorption.

The principles of the PALS method have been previously discussed[12−19] and are only briefly introduced here. In a typical PALS measurement on a thin film, a focused beam of positrons with energy of several keV is implanted into the thin film and forms positronium (Ps, the electron-positron bound state) inside the pores of the film throughout the film thickness. As shown in Figure 1, if Ps is trapped inside the film, the vacuum lifetime of orthopositronium (142 ns) is reduced by annihilation with bound electrons during collisions with the pore surface. Thus, pore size information can be extracted from measuring this shortened lifetime, τ. If the pores are interconnected, some Ps can diffuse out of the film and into the vacuum where it annihilates with its intrinsic lifetime of 142 ns. Thus, PALS can determine whether the pores are interconnected from the telltale vacuum Ps component as a result of Ps diffusing out of the porous film. In this case, however, the annihilation lifetime is not indicative of the average pore size. To measure the pore size for films with connected pores, a nonporous capping layer is needed to prevent Ps out-diffusion from the film. The capping layer traps Ps in the film so that the Ps lifetime is characteristic of the average pore size. Therefore, PALS can be used to measure both open voids and closed pores. Compared with other on-wafer techniques, the PALS method is direct and does not need the adsorption of a probe molecule to obtain pore size, pore size distribution, and pore connectivity information. The sample size required is also relatively small ($\sim$1 cm^2).

All the aforementioned on-wafer methods as well as the off-wafer nitrogen adsorption technique are model-dependent in determining the pore size and pore structure. Comparative studies have been carried out for these on-wafer techniques,[8] and reasonably good agreement has been found among the different techniques. However, none of these techniques have been calibrated against a porous film with a crystallographically determined pore structure (i.e., model-independent). In the present study we have used PALS for the first time to study zeolite low-*k* thin films to obtain pore size and pore connectivity information. The most important goal of this work is to use the crystallographically defined zeolitic pores in the in-situ and spin-on MFI films as a calibration tool for the PALS technique. The PALS method demonstrated here also has significant implications for defects detection in zeolite films for other applications such as zeolite membranes and membrane reactors.

Experimental Section

Films Preparation. PSZ MFI films were prepared by in-situ and spin-on processes as reported previously.[6,7] Briefly, in-situ *b*-oriented MFI films on silicon wafers were prepared by direct crystallization at 165 °C for 2 h in a clear solution with a molar composition 0.32TPAOH/TEOS/165H_2O (TPAOH is tetrapropylammonium hydroxide and TEOS is tetraethyl orthosilicate). For the spin-on MFI film, a nanoparticle suspension with a range of particle sizes was synthesized using a clear solution of molar composition 1TPAOH/2.8SiO_2/22.4EtOH/40H_2O. The clear solution was aged in a capped plastic bottle for 3 days at room temperature followed by crystallization at 80 °C for 5 days. During the whole process constant stirring was provided. The nanoparticle suspension obtained was then centrifuged at 5000 rpm for 20 min and passed through a 0.2 μm PTFE filter to remove large particles. Then, the suspension was spun on a low-resistivity silicon wafer at 3300 rpm with an acceleration of 1275 rpm/s for 20 s at room temperature on a Laurell spin-coater (model WS-400A-6NPP/LITE). Both in-situ and spin-on films were calcined at 450 °C for 2−9 h in air to remove the organic structure-directing agent (i.e., TPA).

Characterization Methods. The pore size and pore interconnectivity of the film samples were examined by PALS at room temperature. The details of the instrument setup and measurement methods appeared elsewhere.[12−19] PALS spectra with 10^7 events were acquired at room temperature with a channel plate start-fast plastic scintillator stop lifetime system with a resolution of 500 ps. The samples were studied at four positron beam implantation energies (2, 3, 5, and 8 keV) to search for any depth-related heterogeneity, and the POSFIT program was used for data fitting. If the samples were determined to have connected pores, an 80 nm silica cap was sputter-deposited to confine Ps to the pores in the film, which allowed the measurement of the average pore size in an interconnected porous network.[16] To deduce the pore size from the o-Ps lifetime, the rectangular Tao−Eldrup (RTE) model is used.[17] As a standard, the Tao−Eldrup (TE) model has been used to calculate the pore size for the micropores ($R < 2$ nm).[13] The TE model treats the o-Ps as a quantum particle with twice the electron mass trapped in the ground state of an infinite spherical potential wall. The self-annihilation of o-Ps ($\tau = 142$ ns) inside the pore is reasonably neglected, while the o-Ps is assumed to have the spin-averaged Ps lifetime (0.5 ns) within a distance ΔR of the pore walls. This is called the "pick-off" quenching annihilation due to interaction of the o-Ps with the electron cloud of the molecules surrounding the pore. Therefore, the overall annihilation rate ($\lambda = 1/\tau$) is the spin-averaged Ps lifetime weighted by the quantum mechanical probability of the o-Ps existing in the ΔR region and is given by

$$\lambda_{TE}(R) = \frac{1}{0.5\ \text{ns}}\left[1 - \frac{R}{R+\Delta R} + \frac{1}{2\pi}\sin\left(\frac{2\pi R}{R+\Delta R}\right)\right]$$

The rectangular Tao−Eldrup (RTE) model extends the TE model to much broader applications (e.g., elongated pores and large mesopores with R>2 nm) by including the possibility of o-Ps being in an excited state of the potential well and weighted by the Boltzmann population distribution.[17] Inclusion of faster decaying excited states in the well is crucial to calibrating mesopore size from fitted Ps lifetime. Readers are directed to ref 17 for information regarding the details of the RTE model.

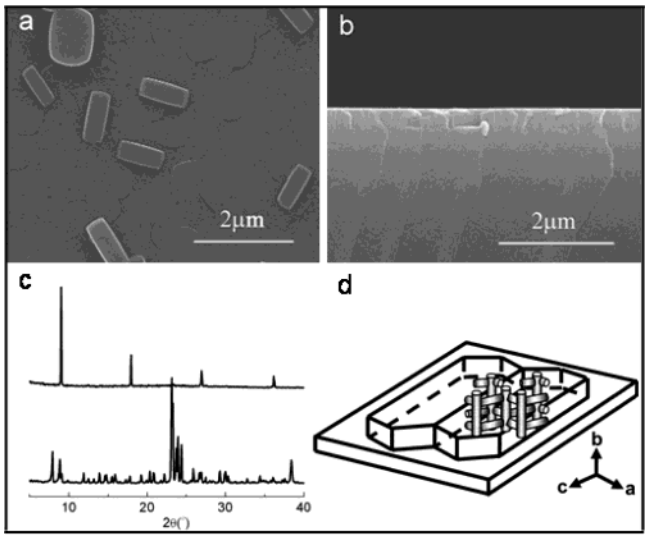

Figure 2. Scanning electron micrographs of (a) an in-situ pure silica zeolite (PSZ) MFI film, (b) cross-sectional view of (a), (c) XRD patterns of bulk MFI powder (bottom) and a *b*-oriented MFI film (top), and (d) schematic of the pore structure of *b*-oriented MFI crystals.

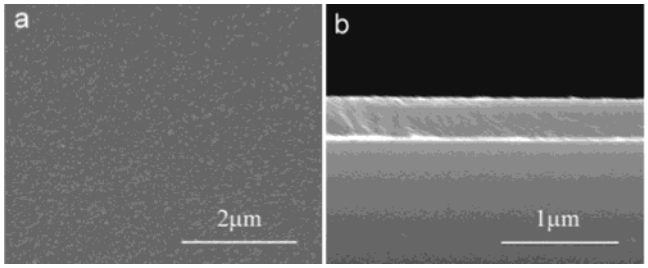

Figure 3. Scanning electron micrographs of (a) a spin-on pure silica zeolite MFI film and (b) cross-sectional view of (a).

The pore size and pore size distribution were also measured by N_2 adsorption on powder samples corresponding to the in-situ and spin-on films (Micromeritics ASAP 2010), and the bulk powders were calcined under the same condition as films before N_2 adsorption measurement. Before measurement, the samples were degassed at 350 °C overnight at 10^{-4} Torr to remove moisture and other adsorbates.

Results and Discussion

The top and cross-section SEM micrographs of an in-situ pure silica zeolite (PSZ) MFI film (Figure 2a,b) show that the in-situ film has a monocrystal-thick structure consisting of *b*-oriented MFI crystals (*b*-axis perpendicular to the substrate). Within the *b*-oriented MFI film, the straight channels in the *b*-direction of the MFI crystals are perpendicular to the substrate and through the whole film thickness. This preferred orientation was confirmed by X-ray diffraction (XRD) (Figure 2c, top). As shown, the XRD pattern of the *b*-oriented MFI film has only (020), (040), (060), and (080) diffraction lines, which are clearly different from those of the randomly oriented powder sample (Figure 2c, bottom). This preferred orientation is illustrated schematically in Figure 2d. The SEM images of the spin-on film are shown in Figure 3. The zeolite nanoparticles in the spin-on film are well dispersed over the whole film thickness, and no cracks were observed. Both in-situ and spin-on films are ~0.4−0.5 μm thick.

PALS measurement on uncapped in-situ zeolite film revealed two short-lived positronium (Ps) components τ_1 and τ_2, and the detailed fitting results are given in Table 1. The relatively low intensity of τ_2 and its $1/E$ dependence on beam energy indicates that this component is contributed by backscattered fast Ps formation.[20] τ_1 is the physically meaningful Ps component for the in-situ zeolite films (Table 1), which has a lifetime value in the range 2.5−3.0 ns with an intensity about 20−25%. Assuming a cylindrical pore geometry, this range of lifetimes corresponds to pore diameters[12−14] (and also mean free path) of 0.52−0.58 nm, remarkably close to the pore size of PSZ MFI of ~0.55 nm as determined crystallographically.

TABLE 1: Fitted Short Lifetime Ps Components in the Uncapped In-Situ and Spin-On Film[a]

energy (keV)	lifetime τ_1 (ns)	cylindrical diam (nm)	I_1 (%)	lifetime τ_2 (ns)	I_2 (%)
		In-Situ Films			
2	2.55 ± 0.04	0.53 ± 0.005	25.4	7.3 ± 0.2	3.8
3	2.52 ± 0.01	0.52 ± 0.001	25.5	7.2 ± 0.1	3.1
5	2.77 ± 0.02	0.55 ± 0.003	21.2	8.4 ± 0.3	1.9
8	3.00 ± 0.02	0.58 ± 0.003	18.1	14.0 ± 0.5	0.9
		Spin-On Films			
2	2.93 ± 0.02	0.58 ± 0.003	13.4	8.7 ± 0.1	3.5
3	2.95 ± 0.05	0.58 ± 0.006	13.3	9.5 ± 0.4	2.7
5	3.12 ± 0.01	0.60 ± 0.001	12.5	13.6 ± 0.3	1.9
8	3.14 ± 0.03	0.60 ± 0.004	10.9	14.1 ± 1.0	1.3

[a] The low-intensity second lifetime component is attributed to backscattered Ps and is thus not relevant to the film's micropores.

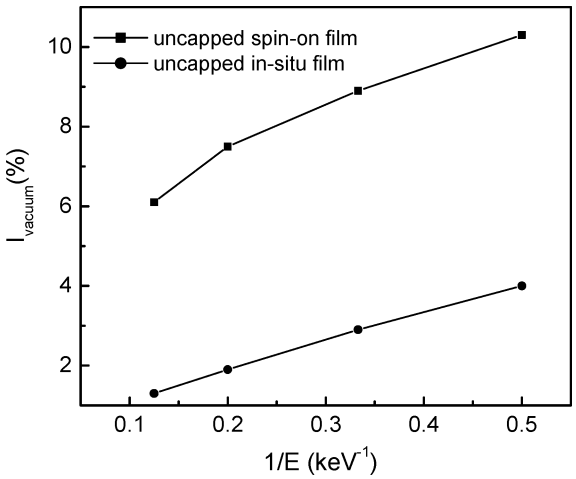

Figure 4. Intensity of the o-Ps component (lifetime 142 ns) escaping in a vacuum for the uncapped spin-on and in-situ films. This in-situ film was measured prior to a degassing anneal that removed absorbed moisture or hydrocarbons that blocked Ps out-diffusion. After annealing the in-situ film the intensity of the 142 ns lifetime increased indicative of Ps out-diffusion.

Ps intensities decaying in a vacuum on the uncapped in-situ and spin-on films are plotted in Figure 4. The Ps intensity of the in-situ zeolite film follows an inverse relationship with the implantation energy and is of low intensity that is in the normally observed intensity range of backscattered Ps. This indicates that the observed vacuum Ps intensity on the in-situ zeolite film is just due to backscattering; no Ps escapes from the pores into vacuum for this film. This suggests that the in-situ zeolite film has closed pores, at least for Ps diffusion. However, it is well-known that the pore channels of MFI interconnect with each other, and no real closure of pores is expected to exist. The explanation appears to be that the micropores contain some minute adsorbed contamination (such as moisture or hydrocarbons) in the pores that effectively blocks Ps diffusion. (Ps is 1000 times lighter than H and does not move atoms in collisions.) This seems to be the case as a separate in-situ film showed copious escaping Ps into vacuum after heat treatment

TABLE 2: Fitted Long Lifetime Ps Components in the Uncapped (Capped) Spin-On Films[a]

energy (keV)	lifetime L_1 (ns)	intensity I_1 (%)	vacuum Ps intensity (%)	cylindrical diam (nm)
2	29.5 ± 0.9	1.8	10.3	
3	33.8 ± 2.0	2.2	8.9	
5	26.2 ± 0.8	2.0	7.5	
8	25.2 ± 2.6	1.3	6.1	
5[b]	47.7 ± 1.2	5.4	2.2	2.65 ± 0.05

[a] Only the capped film lifetime is meaningful in determining the mesopore size. [b] For the capped spin-on film

to 400 °C in a vacuum. Thus, the 0.55 nm micropores in this film are interconnected after all but are easily susceptible to pore blockage by surface contamination.

Similar to in-situ films, two components of short lifetime Ps are fitted on uncapped spin-on films (Table 1). Again, τ_2 is attributed to backscattered fast Ps formation. Values of τ_1 are in the same range as those in the in-situ film, indicating there are micropores with a mean free path around 0.55 ± 0.03 nm in these films too. Besides the two short lifetime Ps components, there is a third Ps lifetime component L_1 detected in the spin-on film, which is associated with mesopores. However, the observed intensity of the L_1 component is relatively low, and the L_1 lifetime is shorter than that measured in the capped sample. Since L_1 intensity and lifetime values are known to be lowered as a result of Ps escaping into the vacuum, the lower intensities of L_1 component together with the higher intensity of Ps annihilating in a vacuum (Figure 4) indicate that these mesopores are interconnected in the spin-on films, through which Ps can freely diffuse out and escape into vacuum. To extract the intrinsic mesopore size, a capping layer of 80 nm SiO_2 was deposited on spin-on films by sputter deposition, and PALS spectra were acquired at 5 keV beam energy (optimum for penetration through the cap and stopping in the zeolite film). The results of long Ps lifetime fitting of capped spin-on films are given in Table 2. The Ps intensity detected in a vacuum decreased from 7.5% (shown in Figure 4) to 2.0% after capping, which indicates that the capping layer blocked the diffusion of Ps out of the film. (The observed 2% Ps intensity in a vacuum is due to the backscattered Ps.) Correspondingly, a much higher mesopore Ps intensity (5.4%) was detected in the film. Furthermore, the fitted lifetime of component L_1 increased to about 47 ns in the capped spin-on film samples, and this lifetime is characteristic of the average size of the mesopores. Using a two-dimensional cylindrical pore model, a diameter and mean free path of 2.6 nm is obtained. Employing a three-dimensional spherical model, the deduced average mean free path in the mesopores is 2.3 nm. As shown from the above results, the spin-on films have both micropores (~0.55 nm mean free path) and open/interconnected mesopores (2.3−2.6 nm) with rather little dependence on the pore models.

Nitrogen adsorption/desorption was also performed on bulk powder samples from the in-situ crystallization process and from drying the nanoparticle suspension from which the spin-on film was prepared. Both materials show very similar micropore size distribution with a pore size around 0.58 nm based on the Horvath−Kawazoe model[21] modified by Foley[22] for cylindrical pores. This is consistent with the thin film PALS results and very close to the well-known pore size of PSZ MFI (~0.55 nm). For the spin-on process nanoparticle suspension, mesopores were observed with a pore size around 2.2 nm based on the Barrett−Joyner−Halenda (BJH) plot, which is once again consistent with the mesopore size/mean free path of 2.3−2.6 nm measured in the actual film using PALS.

In summary, in the present work, pore size and pore structure information on our in-situ and spin-on pure silica zeolite MFI low-*k* films were characterized by PALS. The crystallographically defined zeolitic pores were used as a calibration tool for the PALS technique. The micropore size of 0.52−0.58 nm obtained by PALS is in excellent agreement with the crystallographically defined zeolitic pores (~0.55 nm), showing the applicability of PALS in probing microporous thin film zeolite materials. Also, consistent pore size results were obtained by both PALS and N_2 adsorption techniques. PALS shows further that the mesopores in the zeolite films are open/interconnected. This pore structure information is important for the development of porous low-*k* films. Ideally, the mesopores of the on-chip insulators should be closed cells to reduce moisture uptake, minimize film damage by the reactive plasmas, and prevent diffusion of the metal deposition precursors used by chemical vapor deposition (CVD) and atomic layer deposition (ALD). Moreover, films with closed mesopores may possess other superior properties such as higher mechanical strength and breakdown voltage relative to other materials with the same porosity but with open mesopores. The effects of open micropores in low-*k* materials are not yet fully understood. Considering the presence of open mesopores in our spin-on zeolite films, in our future study, we will attempt to change the open mesopore structure to closed mesopore structure by adjusting the ratio of the zeolite nanocrystal to amorphous silica phase.

Acknowledgment. We thank AMD, Asahi Kasei Corp., NSF (CTS 0404376 and ECS 0100009), and UC-Discovery Grant for financial support.

References and Notes

(1) The International Technology Roadmap for Semiconductors, International SEMATECH, Austin, TX, 2002.
(2) Miller, R. D. *Science* **1999**, *286*, 421−423.
(3) Kondoh, E.; Baklanov, M. R.; Bender, H.; Maex, K. *Electrochem. Solid State* **1998**, *1*, 224−226.
(4) Morgen, M.; Ryan, E. T.; Zhao, J. H.; Hu, C.; Cho, T. H.; Ho, P. S. *Annu. Rev. Mater. Sci.* **2000**, *30*, 645−680.
(5) Jain, A.; Rogojevic, S.; Ponoth, S.; Gill, W. N.; Plawsky, J. L.; Simonyi, E.; Chen, S. T.; Ho, P. S. *J. Appl. Phys.* **2002**, *91*, 3275−3281.
(6) Wang, Z. B.; Mitra, A. P.; Wang, H. T.; Huang, L. M.; Yan, Y. H. *Adv. Mater.* **2001**, *13*, 1463−1466.
(7) Wang, Z. B.; Wang, H. T.; Mitra, A.; Huang, L. M.; Yan, Y. S. *Adv. Mater.* **2001**, *13*, 746−749.
(8) Kondoh, E.; Baklanov, M. R.; Lin, E.; Gidley, D.; Nakashima, A. *Jpn. J. Appl. Phys. 2* **2001**, *40*, L323−L326.
(9) Grill, A.; Patel, V.; Rodbell, K. P.; Huang, E.; Baklanov, M. R.; Mogilnikov, K. P.; Toney, M.; Kim, H. C. *J. Appl. Phys.* **2003**, *94*, 3427−3435.
(10) Baklanov, M. R. M. K. P. *Proceedings−International Conference on Solid-State and Integrated Circuit Technology, 6th, Shanghai, China, Oct. 22−25, 2001* **2001**, *1*, 352.
(11) Wu, W. L.; Wallace, W. E.; Lin, E. K.; Lynn, G. W.; Glinka, C. J.; Ryan, E. T.; Ho, H. M. *J. Appl. Phys.* **2000**, *87*, 1193−1200.
(12) Wang, Y. Y.; Nakanishi, H.; Jean, Y. C.; Sandreczki, T. C. *J. Polym. Sci. Polym. Phys.* **1990**, *28*, 1431−1441.
(13) Eldrup, M.; Lightbody, D.; Sherwood, J. N. *Chem. Phys.* **1981**, *63*, 51−58.
(14) Tao, S. J. *J. Chem. Phys.* **1972**, *56*, 5499−5510.
(15) Gidley, D. W.; Frieze, W. E.; Dull, T. L.; Yee, A. F.; Ryan, E. T.; Ho, H. M. *Phys. Rev. B* **1999**, *60*, R5157−R5160.
(16) Petkov, M. P.; Wang, C. L.; Weber, M. H.; Lynn, K. G.; Rodbell, K. P. *J. Phys. Chem. B* **2003**, *107*, 2725−2734.
(17) Dull, T. L.; Frieze, W. E.; Gidley, D. W.; Sun, J. N.; Yee, A. F. *J. Phys. Chem. B* **2001**, *105*, 4657−4662.
(18) Sun, J. N.; Gidley, D. W.; Hu, Y.; Frieze, W. E.; Ryan, E. T. *Appl. Phys. Lett.* **2002**, *81*, 1447−1449.
(19) Gidley, D. W.; Frieze, W. E.; Dull, T. L.; Sun, J.; Yee, A. F.; Nguyen, C. V.; Yoon, D. Y. *Appl. Phys. Lett.* **2000**, *76*, 1282−1284.
(20) Gidley, D. W.; McKinsey, D. N.; Zitzewitz, P. W. *J. Appl. Phys.* **1995**, *78*, 1406−1410.
(21) Horvath, G.; Kawazoe, K. *J. Chem. Eng. Jpn.* **1983**, *16*, 470−475.
(22) Saito, A.; Foley, H. C. *Microporous Mater.* **1995**, *3*, 531−542.